

Stochastic model of template-directed elongation processes in biology

Authors:

Maria J. Schilstra^{1,*}

Chrystopher L. Nehaniv^{1,2}

¹ Biocomputation Research Group, Science & Technology Research Institute, and ² Adaptive Systems Research Group, School of Computer Science. University of Hertfordshire, College Lane, Hatfield AL10 9AB, UK

* Corresponding author:

Maria J. Schilstra

Biocomputation Research Group, STRI

University of Hertfordshire

College Lane

Hatfield AL10 9AB, UK

Email M.J.1.Schilstra@herts.ac.uk

Tel +44 (0)1707 281376

Fax +44 (0)1707 284185

Summary

We present a novel modular, stochastic model for biological template-based linear chain elongation processes. In this model, elongation complexes (ECs; DNA polymerase, RNA polymerase, or ribosomes associated with nascent chains) that span a finite number of template units step along the template, one after another, with semaphore constructs preventing overtaking. The central elongation module is readily extended with modules that represent initiation and termination processes. The model was used to explore the effect of EC span on motor velocity and dispersion, and the effect of initiation activator and repressor binding kinetics on the overall elongation dynamics. The results demonstrate that 1) motors that move smoothly are able to travel at a greater velocity and closer together than motors that move more erratically, and 2) the rate at which completed chains are released is proportional to the occupancy or vacancy of activator or repressor binding sites *only* when initiation or activator/repressor dissociation is slow in comparison with elongation.

Keywords

Replication, transcription, translation, initiation, elongation, termination, template-directed, Petri-net, semaphore, stochastic, congestion, kinetics

Introduction

Replication, transcription, and translation are template-directed processes in which linear DNA, RNA, or polypeptide (protein) chains are synthesized on the basis of the information stored in existing DNA (for replication and transcription) or RNA (for translation). All three processes occur in three major stages: initiation, elongation, and termination. During initiation, a polymerase, a molecular motor that catalyzes the polymerization, is recruited to the initiation site on the template, and performs the first step in the synthesis of new polymer chains. Each process requires its own kind of polymerase: DNA polymerase for replication, RNA polymerase for transcription, and ribosomes for translation. Polymerases use some of the energy that is liberated upon addition of a new unit to the nascent chain to move unidirectionally along the template.

Initiation may involve the binding of additional proteins called initiation factors (IFs) to specific sites in the vicinity of the initiation site. There are many types of IFs, with different affinities for their specific binding sites on the various templates, and different effects on initiation. Some have a stimulatory effect, increasing the initiation rate; others act as repressors that slow down or block the initiation process.

In the elongation phase, the polymerase moves along the template, adding new units one by one to the nascent chain. A polymerase-nascent chain complex that is moving along the template is called an elongation complex (EC). Each polymerase step consists of (at least) two discernible sub-steps. The elongation reaction, in which a new unit is attached to the end of the chain, is a multistep process that may take milliseconds to complete, whereas the step that follows, translocation (the actual movement of the EC to the next unit on the template) is over much more quickly. As a result, the EC appears to dwell for a finite amount of time in a particular position, and then, almost instantaneously, moves forward to the next position. ECs (i.e. the polymerase-nascent chain residing somewhere on the template) tend to be very stable, with lifetimes that may be measured in hours.

However, when an EC reaches a stop site --a specific nucleotide sequence-- the production process enters the termination stage, in which the EC sheds the completed chain and the polymerase dissociates from the template.

Termination may require the help of proteins called termination factors, but in some cases the polymerase has such a weak affinity for the stop site that the complex dissociates rapidly without further assistance (see e.g. Lodish, 2004).

As IFs or IF complexes have finite affinities for their binding sites on the template, it is often assumed that the level of activation or repression, and consequently the replication, transcription, or translation rates themselves, are proportional to the average occupancy level (fractional saturation) of these sites (see e.g. Ackers, 1982,

Alon, 2006, Shea, 1985). Dynamic models based on these assumptions do not take into account that 1) IF-template complexes have a finite lifetime, 2) polymerase recruitment and assembly¹ takes time, and 3) can only occur at vacant initiation sites; 4) ECs span several nucleotides, and 5) cannot overtake each other.

A much more sophisticated approach to the modelling of mRNA-directed protein synthesis was presented in the late 1960s (MacDonald, 1968, MacDonald, 1969). This mean-field approach takes into consideration points 3, 4, and 5 above, and formed the basis for several in-depth analyses of template-directed processes (see e.g. Garai, 2009, Heinrich, 1980, Zouridis, 2007, and references therein).

Here, we present a discrete, stochastic model of biological linear template-directed processes that is capable of taking into account all five conditions above. The basic model introduced here is in some respects less comprehensive than some of the earlier models, but is easily extended to include more detail. Because of the addition of semaphores (Dijkstra, 2002) to the basic particle-hopping scheme that describes the elongation process, the model can be implemented quite straightforwardly in, for example, multi-purpose stochastic Petri-net simulators, without the need for model-specific “hard-wiring” of conditional statements in software code. We demonstrate the use of this model in the exploration of stochastic phenomena such as noise distribution and dynamic effects that are beyond the reach of mean-field and other deterministic models.

Model

The model, shown in Figure 1, is depicted as a Petri net (Petri, 1962). The Petri net notation is eminently suitable for representing biochemical reaction systems, as it emphasizes the discrete nature of molecular interactions, and draws attention to the structure of, and dependencies within interaction networks. If the rules of chemical kinetics are used to characterize dynamic tendencies within the network, the Petri net notation is equivalent to the standard chemical reaction notation, and can be used to automatically derive the stoichiometry and rate equations that are used to compute the temporal development of chemical reaction systems (see, e.g., Schilstra, 2009, Wilkinson, 2006).

The Petri net terminology is somewhat idiosyncratic, and fairly different from the standard vocabulary used to describe chemical reaction systems. In brief, a Petri net is a bipartite directed graph, in which nodes usually indicated as *places* are connected to nodes that are generally called *transitions*. Places that are connected to a transition via input arcs, arcs pointing toward the transition, are referred to as the transition’s input places; arcs

¹ Polymerases consist of several subunits that assemble at or near the initiation site to form a fully functional motor. After dissociation from the termination site, the motor disassembles into its constituent subunits.

pointing toward places are output arcs that connect a transition's output places. The nodes in Figure 1 are grouped in *layers* whose sole function here is to facilitate interpretation of the model. Places are containers for *tokens*, and represent the system's state, whereas transitions are responsible for the system's dynamics by *firing* and changing the Petri-net's *marking* (token distribution). When a transition fires, tokens are removed from its input places, and new tokens deposited in its output places. Each arc has a *weight* that determines how many tokens are removed and deposited into its associated place. A transition is *enabled*, i.e., allowed to fire, if and only if the number of tokens in each of its input places is equal to or greater than the weights of their associated input arcs. In the model presented here, all arc weights are 1. Thus, when the token distribution in the Petri net model is as illustrated in Figure 1, transition $tE_{4,5}$ is enabled as its input places E_4 and T_6 contain a token each, whereas $tE_{1,2}$ is disabled because E_1 is empty. Place A_1 and transition $tIni$ form a self-loop: a place that is connected to a transition via both an input and an output arc. Firing of $tIni$ will therefore remove as well as deposit a token in A_1 , leaving the state of A_1 unchanged. However, $tIni$ is enabled only if A_1 contains a token. A_1 , therefore, represents some condition that must be fulfilled for initiation to occur.

The model is interpreted as follows. The places in the T layer represent all positions on the template that can be occupied by the EC, i.e. the *track*. Each track position contains at most one token; if the token is present, the position is free, if not, the position is occupied by the EC. Transition $tIni$ in layer A represents the entire transcription *initiation* process, in which RNAP is assembled on, and released from the promoter. Note that $tIni$ is enabled only when places T_1 , T_2 , and A_1 each contain a token. This means that an EC can only be assembled and released if the first two positions on the track, T_1 and T_2 , are vacant. Place A_1 represents what we will refer to as the *activation condition*, which must be fulfilled for transcription to be initiated. A_0 and A_1 may be interpreted as the occupancy state of a regulatory site on the gene, and $tA_{0,1}$ and $tA_{1,0}$ as the processes in which the activator or repressor molecule associate with or dissociate from the regulatory site. The transitions in layer E symbolize the consecutive translocation steps in the elongation process, and the places in E represent nascent transcripts of increasing lengths. Finally, transition $tTerm$, in layer C, represents the entire termination process, in which the EC dissociates from the track and sheds its transcript. Place C_0 merely acts as a counter for completed transcription rounds (or finished transcripts).

Dynamics

The model structure and the initial token distribution constrain the total number of possible trajectories (development of the system's marking), whereas the firing rules or firing propensities associated with individual

transitions determine the likelihood that particular trajectories are followed. In the situation in which the track is empty, and the activation condition fulfilled (one token in \mathbf{A}_1), only \mathbf{tIni} and \mathbf{tA}_{10} are enabled. Upon firing of \mathbf{tIni} , a token will appear in \mathbf{E}_1 , representing the presence of an EC containing a nascent RNA chain of length 1. Because \mathbf{tIni} is connected to \mathbf{A}_1 via a self-loop, \mathbf{A}_1 regains its token and the activation condition remains fulfilled, but the tokens in \mathbf{T}_1 and \mathbf{T}_2 disappear, as sites 1 and 2 on the track are now occupied. Because \mathbf{T}_1 and \mathbf{T}_2 are empty, \mathbf{tIni} is disabled, but \mathbf{tE}_{12} is now enabled, as both of its input places, \mathbf{T}_3 and \mathbf{E}_1 , contain a token. The next transition that will fire is, therefore, \mathbf{tE}_{12} , and upon its firing the tokens in \mathbf{E}_1 and \mathbf{T}_3 will disappear, but new tokens will appear in \mathbf{T}_1 and \mathbf{E}_2 , and \mathbf{tE}_{23} will become enabled. After \mathbf{tE}_{23} has fired and its associated token redistribution has taken place, \mathbf{T}_1 and \mathbf{T}_2 will both contain a token and \mathbf{tIni} will become enabled once again. This token movement is interpreted as the directed motion of one EC down the track. Once the first two positions on the track have been vacated, two transitions (\mathbf{tIni} and $\mathbf{tE}_{3,4}$) are enabled, and there is a choice of two possible events: a new initiation, or an elongation step. Independent of the transition firing pattern that results in the apparent motion of ECs, \mathbf{tA}_{10} may also fire, thereby negating the activation condition, and preventing \mathbf{tIni} from firing at all, until the activation condition is restored by the firing of \mathbf{tA}_{01} . Firing of any transition (but \mathbf{tTerm}) will enable or disable other transitions, and advance the system. After some time, tokens will begin to appear in \mathbf{C}_0 , one by one, each registering the successful completion of a transcription round. Note that the wiring of the nodes in layers E and T prevent deposition of new tokens in places that already contain one. In fact, the places \mathbf{T}_{j+2} act as semaphores (Dijkstra, 2002), allowing ECs to “pass” position j one at a time, preventing them from overtaking each other, and making them wait until the one in front has moved on. Thus, Figure 1 depicts a situation in which three different elongation complexes are present on the template. The oldest one occupies position N only, and is about to complete its run. The newest complex occupies positions 4 and 5, and can move to positions 5 and 6. Translocation of the second oldest complex, occupying positions $N-2$ and $N-1$, is blocked until the complex in position N has moved out of the way. The number of tokens in \mathbf{C}_0 indicates that three transcription rounds have already been completed.

Model extension

In the model shown in Figure 1 the track is 9 units long ($N = 9$), with each EC spanning two consecutive positions ($L = 2$). The track length, N , and the EC span, L , in the basic model are changed by inserting or deleting the required number of places and transitions in the T and E layers (to change N), and performing the appropriate rewiring:

1. **tIni** - input from \mathbf{T}_1 to \mathbf{T}_L , output to \mathbf{E}_1
2. **tTerm** - input from \mathbf{E}_N , output to \mathbf{T}_N
3. **tE_{j,j+1}** ($0 < j < N$) - input from \mathbf{E}_j , output to \mathbf{E}_{j+1} and \mathbf{T}_j
4. **tE_{j,j+1}** ($0 < j < (N - L)$) - input from \mathbf{T}_{j+L} , creating the semaphores

Because of its modular nature (Track/Elongation, Initiation, Termination), the model is readily extended to incorporate phenomena not present in the basic model. For instance, to model the possibility of the EC dissociating from the track prematurely, a set of new transitions, **tD_j**, symbolizing EC dissociation from position j on the template, may be wired via input arcs to \mathbf{E}_j and via output arcs to $\mathbf{T}_j \dots \mathbf{T}_{j+L-1}$, so that whenever a token appears in \mathbf{E}_j , not only **tE_{j,j+1}**, but also **tD_j** gets enabled. Models in which m intermediate steps precede the translocation in **tE_{j,j+1}** may be obtained by inserting linear chains of m [place-input arc-transition-output arc] units between **tE_{j,j+1}** and \mathbf{E}_{j+1} , connecting the first place in the chain via an output arc to **tE_{j,j+1}**, and the last output arc to \mathbf{E}_{j+1} . Even though there is no restriction to the number of tokens in any of the places in such a chain, again the wiring of the nodes surrounding it prevent the presence of more than one token inside the chain at any time. More intricate initiation schemes may be realized by adding parallel initiation transitions, to mimic regulation by alternative initiation complexes, or by including more detail in the initiation complex dynamics (e.g. making its lifetime dependent on the concentrations of one or more initiation factors). The initiation process itself, which, in the model used here, is represented by a single transition (**tIni**), and characterized by a single rate constant (k_{ini}) may be extended to include stages in the assembly of the polymerase. Likewise, the termination process may be extended to include more intricate details of termination factor activity.

Dynamics simulation

In the approach discussed in this paper, transitions are allowed to fire stochastically at an average frequency proportional to the product of the number of tokens in their input places (thus, the firing probability of a disabled transition is zero). Each transition j is assigned a rate constant k_j , and its firing propensity (or flux) J_j computed as

$$J_j = k_j \prod_{i=1}^{n_j} x_{j,i} \quad (1)$$

Here $i = 1$ to n_j enumerate all n_j inputs to the j^{th} transition, and $x_{j,i}$ represents the number of tokens in its i^{th} input place². The development of the Petri net marking over time is simulated using a variant of Gillespie's First Reaction algorithm (Gillespie, 1977). In the First Reaction algorithm, a firing time interval Δt_j is computed for each transition j from its current flux J_j and a random number, p_j , chosen from a uniform distribution between zero and one ($0 \leq p_j < 1$) for each transition.

$$\Delta t_j = -\frac{\ln(1-p_j)}{J_j} \quad (2)$$

The transition for which the smallest time interval is obtained (Δt_{\min}) is selected to fire at time $t + \Delta t_{\min}$, after which the simulation time t is set to $t + \Delta t_{\min}$. This process is repeated until a pre-set simulation time has been exceeded or until no further token rearrangement is possible.

The dynamic behaviour of the model was assessed using NetBuilder⁷, an open-source package for simulation (stochastic, deterministic, and hybrid) of biochemical reaction networks. NetBuilder⁷ includes graphical and (Python) scripting interfaces for specifying the reaction networks as Petri-net models. To create the model described here, the scripting interface was used because of its greater flexibility and expressive power. To perform the simulations, NetBuilder⁷ converts the Petri-net model in rate and state vectors, and pre- and post-incidence matrices, which are then used to advance the system, as described, for instance, in Wilkinson (2006, chapter 2). NetBuilder's stochastic simulator, which was used in the simulations described below, implements a variant of Gillespie's First Reaction algorithm, in which a priority queue of enabled transitions is constructed from a state dependency matrix and maintained (the so-called Next Reaction Method, Gibson, 2000) to improve efficiency.

In all simulations described here, the track N was 20 times the size of the EC span L ($N = 20 \times L$). Each simulation round was started with a token in \mathbf{A}_1 (activation condition fulfilled), and one token in each of $\mathbf{E}_1 \dots \mathbf{E}_N$ (empty track). The values of the rate constants $k_{E_j, j+1}$ associated with the translocation transitions $tE_{j, j+1}$ were all given an identical value, k_E . The value of L determined value assigned to k_E : $k_E = L \times 1.0$ per time unit, so that, in the absence of any hindrances and on average, the EC moves L positions in one time unit, takes 20 time units to move down the full track.

² In fact, Equation 1 represents the law of mass action

Results and Discussion

Effect of EC dispersion on the production rate In a system in which the activation condition is always fulfilled ($k_{10} = 0$), and release of the assembled EC onto the track, determined by k_I , is not limiting (here $k_I = 10.0$), the rate at which new rounds start (the actual initiation rate) depends on the span L of the EC. Figure 2 compares the time trajectories of a group of 20 ECs, one group with $L = 1$, the other with $L = 16$, as they move from down the track from position 1 to position $20 \times L$. In both cases, the first EC moves unhindered --albeit somewhat erratically-- along an open track. However, owing to relatively slight random differences in velocity, the next one occasionally runs into the one that was initiated first, and then has to wait until it can move forward. This slows down its overall velocity, which has subsequent effects on the ECs that follow. It is immediately clear, however, that the ECs with the larger span move much more smoothly: their dispersion (deviation from a straight line) is significantly smaller. The difference in uniformity of motion is expected, as movement over L is a single-step process for $L = 1$, but a 16-step sequential process if L spans 16 positions, with time interval between individual steps exponentially distributed. The average time required for the EC to complete L sequential steps with (equal) rate constants k_E obeys a gamma distribution (Gibson, 2000) with a mean of $L/k_E = 1.0$ for both values of L , but a standard deviation of $\sqrt{L/k_E^2}$ equalling 1.0 for $L = 1$ (a gamma distribution for $L = 1$ is an exponential distribution), but only 0.25 for $L = 16$. In all cases, a steady state, where all ECs move at the same average velocity, appears to be reached quickly, but we routinely left the first 10 initiation and termination events out of the analysis to ensure that transient effects were not incorporated in the statistics.

As a result of the difference in uniformity of motion, the average distance between the ECs on the track, and therefore the average interval between consecutive initiation and termination events, Δ_I and Δ_T , is significantly smaller for $L = 16$ than for $L = 1$: 1.4 ± 0.2 (initiation) and 1.4 ± 0.5 (termination) time units for $L = 16$ against 3.7 ± 2.4 (initiation) and 3.7 ± 2.6 (termination) time units for $L = 1$. Figure 2c shows that Δ_I and Δ_T , as well as their variance σ_I and σ_T , decrease gradually to their limiting value of one time unit as L increases. The reciprocal of Δ_T is the rate at which complete chains are produced (from here on referred to as the production rate, ν_p), which is 0.3 ± 0.2 per time unit for $L = 1$, and 0.9 ± 0.2 for $L = 64$. Another measure for the efficiency of the process is the average velocity V at which an EC completes an initiation-elongation-termination round, computed from the time interval between its initiation and termination. If an EC has to wait frequently until its forerunner has moved out of the way, its average velocity will be lower than when it can move unhindered.

Thus, V depends on the density ρ of ECs on the track. The value of ρ was varied by logarithmically increasing the initiation frequency k_I from 0.1 to 10.0, and computed from the termination frequency ν_P ($\rho = \nu_P / \nu_P^{max}$, where ν_P^{max} is the maximum value of ν_P , 1.0). Figure 2d shows that V is close to its maximum value, 1.0, at low densities ($\rho < 0.1$) but decreases for all values of L investigated, until a maximum density is reached. As expected, ECs that move more smoothly achieve higher maximum densities and velocity.

Note that above we have compared ECs that, unhindered, travel their span L , rather than one position, in one unit of time. It follows from Figure 2c that the maximum density of small ECs on a track of a particular length N will always be greater than that of larger ones, irrespective of the level of congestion. However, results similar to the above were obtained with models for which $L = 1$, but in which each translocation step (movement by one position) consists of multiple consecutive reactions.

Relationship between activator or repressor binding site occupancy and production rate

As stated above, the activation condition may be interpreted as the instantaneous occupancy of the initiation activator or repressor binding site (true indicates a bound activator, or unbound repressor). The *average or fractional occupancy* over time of the binding site, Φ , is modulated by keeping the firing rate of \mathbf{tA}_{10} , k_{I0} , constant and varying that of \mathbf{tA}_{01} , k_{0I} :

$$\Phi = \frac{k_{0I}}{k_{0I} + k_{I0}} \left(= \frac{[A]/K_d^A}{1 + [A]/K_d^A} \quad \text{or} \quad = \frac{1}{1 + [R]/K_d^R} \right) \quad (3)$$

Thus, Φ is dimensionless and varies between 0 (for $k_{0I} = 0$) and 1 (for $k_{I0} = 0$). Inside the brackets is a possible interpretation of k_{0I} and k_{I0} , where $[A]$ and $[R]$ are the concentrations of an activator A or repressor R, and K_d^A and K_d^R are the dissociation equilibrium constants for the simplest possible activation or repression scenarios ($B + A \rightleftharpoons AB$ (token in \mathbf{A}_1) or $B + R \rightleftharpoons AR$ (token in \mathbf{A}_0), where B is the binding site, and $[A], [R] \gg 1$). The *lifetime* of the activated state (the average time it exists before becoming inactivated), τ_{A1} , is equal to $1/k_{I0}$, and is changed, without affecting Φ , by proportionally changing k_{0I} and k_{I0} . To explore the relationship between regulator site occupancy and production rate, we compare the dynamics of a system in which both k_I and k_{I0} are fast with respect to the elongation rate k_E with systems in which one is slow and the other fast. Systems in which the value of k_I is large (as compared with k_E/L) have *efficient initiation*: provided the initiation condition remains fulfilled, a new EC is ready to start elongating as soon as the previous one has moved out of the way. This is not the case in systems in which k_I is relatively small. Systems in which the lifetime of the activated state, $1/k_{I0}$, is

short are *responsive* to changes in activator or repressor concentrations: when these concentrations change, Φ can adapt rapidly to the new condition. If the average lifetime of the activated state is long, adaptation will take much longer.

Figure 3 shows the results obtained for three extreme parameter sets, S1, S2, and S3. In S1, a responsive system in which initiation is efficient, the observed production rate increases non-linearly with the regulatory site occupancy, reaching a plateau at $\Phi \approx 0.4$. When the plateau is reached, the standard deviation decreases to approximately 30% as the intervals between successive initiations become more regular. The trajectory in panel c, in which the activation state and **Uni** firing events are plotted over a period of 15 time units, reveals that, even though the activation condition is only true for 50% of the time, the rapid alternation of “on” and “off” states quickly creates new opportunities for new production rounds to begin once the previous EC has moved on. However, if the activation complex is less dynamic, as in S2, or if the initiation system is not able to quickly make use of opportunities to release a new EC, as in S3, the production rate becomes proportional to Φ . In S2, initiation is clustered inside the long periods in which the activation condition is true, and the completed linear chains leave the track in bunches. Although owing to the high efficiency of the initiation process the intervals between initiations within a cluster are regular, the intervals between the clusters are not, so that the overall standard deviation on the observed production rate is very large (approaching 200% at $\Phi = 0.5$ in S2). In S3, on the other hand, initiation is limiting and will only take a fraction of the opportunities that arise. As a result, initiation events are exponentially distributed, and the observed production rate and its standard deviation have the same value. Thus, S2 and S3 respond proportionally to changes in Φ . Of course, the fact that, in most activator or repressor binding scenarios, Φ is non-linearly dependent on the actual activator or repressor concentrations adds an extra layer of non-linearity. As the initiation process initiation is much more efficient in S2 than in S3, S2 achieves the greater production rate. However, S2 cannot respond as rapidly to abrupt “regime” changes, changes in activator or repressor concentrations in response to, e.g., received signals. Unless a bound activator or repressor molecule is *actively* removed (which costs energy), the activated or repressed state may extend unpredictably long into the new regime. S1, on the other hand, will respond rapidly, but is over a large concentration range relatively insensitive to changes in activator or repressor concentrations.

Conclusion

Earlier models of template directed biological production processes are based on particle hopping schemes in which the forward hopping probability is proportional to the average EC density on each position of the track.

The use of semaphores --which represent empty track positions and prevent EC from overtaking each other-- in the model presented here simplifies the modelling procedure, and obviates the need for estimates of local density. The visual nature of Petri-nets combined with the simple concept behind the stochastic First Reaction method (Gillespie, 1977) help understanding the model and facilitate the interpretation of its complex dynamics. These aspects may also encourage further analysis and the derivation of analytical expressions for observables such as steady state flux and EC density, and comparison of the outcome with the results of earlier studies.

Acknowledgement

MJS thanks Prof. Wolfgang Marwan, Max Planck Institute for Dynamics of Complex Technical Systems, Magdeburg, Germany, for introducing her to Petri-net modelling. This work was funded in part by a Wellcome Trust Functional Genomics Development Initiative grant (ref. 072930/Z/03/Z).

References

- Ackers, G.K., Johnson, A.D., Shea, M.A., 1982. Quantitative model for gene regulation by lambda phage repressor. *Proceedings of the National Academy of Sciences USA* 79, 1129-1133.
- Alon, U., 2006. *An introduction to systems biology. Design principles of biological circuits*, Chapman & Hall/CRC, London.
- Dijkstra, E.W. 2002 Cooperating sequential processes, in *The origin of concurrent programming: from semaphores to remote procedure calls*, Springer-Verlag New York, Inc., pp 65-138.
- Garai, A., Chowdhury, D., Ramakrishnan, T.V., 2009. Fluctuations in protein synthesis from a single RNA template: Stochastic kinetics of ribosomes. *Physical Review E* 79, 011916-011916.
- Gibson, M.A., Bruck, J., 2000. Efficient exact stochastic simulation of chemical systems with many species and many channels. *J. Phys. Chem. A*. 104, 1876-1889.
- Gillespie, D.T., 1977. Exact stochastic simulation of coupled chemical reactions. *J. Phys. Chem.* 81, 2340-2361.
- Heinrich, R., Rapoport, T.A., 1980. Mathematical modelling of translation of mRNA in eucaryotes; steady states, time-dependent processes and application to reticulocyttest. *Journal of Theoretical Biology* 86, 279-313.
- Lodish, H., Berk, A., Matsudaira, P., Kaiser, C.A., Krieger, M., Scott, M.P., Zipursky, S.L., Darnell, J., 2004. *Molecular Cell Biology*, 5th ed., W. H. Freeman & Company, New York, NY.
- MacDonald, C.T., Gibbs, J.H., Pipkin, A.C., 1968. Kinetics of biopolymerization on nucleic acid templates. *Biopolymers* 6, 1-25.
- MacDonald, C.T., Gibbs, J.H., 1969. Concerning the kinetics of polypeptide synthesis on polyribosomes. *Biopolymers* 7, 707-725.
- Petri, C.A., 1962 Kommunikation mit Automaten, *Schriften des IIM Nr. 2*, in Institut für Instrumentelle Mathematik, Bonn
- Schilstra, M.J., Martin, S.R. 2009 Simple Stochastic Simulation, in *Methods in Enzymology* (Michael, L.J., Ludwig, B., Eds.), Academic Press, pp 381-409.
- Shea, M.A., Ackers, G.K., 1985. The OR control system of bacteriophage lambda : A physical-chemical model for gene regulation. *Journal of Molecular Biology* 181, 211.
- Wilkinson, D.J., 2006. *Stochastic Modelling for Systems Biology*, Chapman & Hall/CRC, London, UK.
- Zouridis, H., Hatzimanikatis, V., 2007. A Model for Protein Translation: Polysome Self-Organization Leads to Maximum Protein Synthesis Rates. *Biophysical Journal* 92, 717-730.

Figure Legends

Figure 1. Petri-net model of a biological template-directed linear production process, such as DNA replication or transcription, or mRNA translation. Open circles, places; black or grey disks inside places, tokens; rectangles, transitions (open: disabled, grey: enabled); arrows, arcs; rounded rectangles, layers. T, DNA template layer; E, elongation layer; A, activation/initiation layer; C, completion (termination) layer. The N places in layers E and T are numbered E_1, E_2, \dots, E_N , and T_1, T_2, \dots, T_N ; the (unlabeled) transitions in E and A are identified as $tE_{1,2}, tE_{2,3}, \dots, tE_{N-1,N}$, and $tA_{0,1}$ and $tA_{1,0}$, respectively. Rate constants associated with $tIni$, $tTerm$, $tA_{0,1}$, $tA_{1,0}$, and $tE_{j,j+1}$ are named k_I, k_T, k_{0I}, k_{10} , and $kE_{j,j+1}$, respectively.

Figure 2. Effect of elongation complex (EC) span L on transcription rate. The track length was $20 \times L$, and the elongation rate k_E was L positions per unit of time in all simulations. The initiation rate (and thus the EC density) was maximal in all simulations except the ones in panel d. a, b: trajectories of the front of 20 ECs of span 1 and 16, respectively; note the different time scales. c: Average time intervals at steady state between initiation (circles) and termination events (squares), and their standard deviation (wider and narrower error bars for initiation and termination, respectively). d: Average steady state EC velocity (V) as a function of EC density on the track (ρ), for EC spans of 1, 4, and 16 positions. Variation in density was achieved by varying k_I .

Figure 3. Mean observed steady state production rate (number of linear chains completed per unit of time, a) and its standard deviation (b) as a function of average activator binding site occupancy Φ (fraction of time the activation condition is true), and typical trajectories at $\Phi = 0.5$ (c) for S1, a responsive system that has efficient initiation (circles; $k_I = 10$ and $k_{10} = 10$ per time unit), S2, an unresponsive system with efficient initiation (triangles; $k_I = 10, k_{10} = 0.1$), and S3, a responsive system with inefficient initiation (squares; $k_I = 0.1, k_{10} = 10$). All systems had an EC span L of 16 positions; a track length N of $20 \times L$ (320 positions), and elongation rate constant k_E of L positions per time unit. Statistics were obtained from at least 300 full transcription rounds per data point. Standard deviations were computed from the intervals between successive initiations. Solid lines in a and b are inserted solely to guide the eye. Solid lines in c show the activation condition (low, false, high, true); crosses indicate where a new transcription round is initiated ($tIni$ firing).

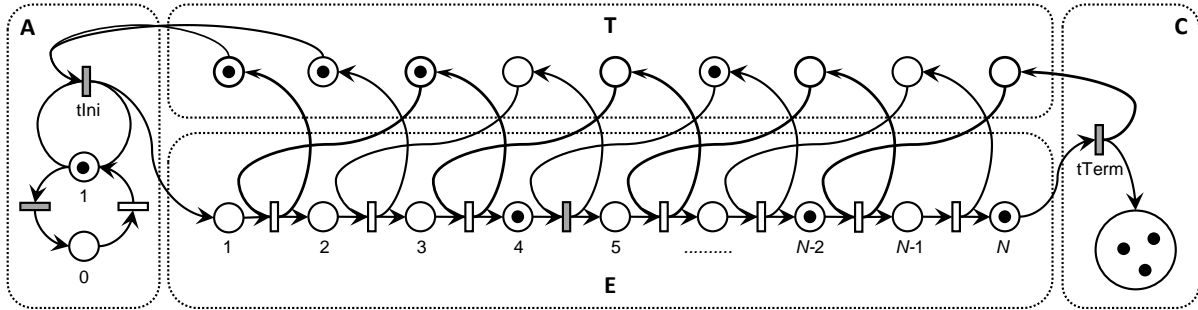


Figure 1. Petri-net model of a biological template-directed linear production process, such as DNA replication or transcription, or mRNA translation. Open circles, places; black or grey disks inside places, tokens; rectangles, transitions (open: disabled, grey: enabled); arrows, arcs; rounded rectangles, layers. T, DNA template layer; E, elongation layer; A, activation/initiation layer; C, completion (termination) layer. The N places in layers E and T are numbered E_1, E_2, \dots, E_N , and T_1, T_2, \dots, T_N ; the (unlabeled) transitions in E and A are identified as $tE_{1,2}, tE_{2,3}, \dots, tE_{N-1,N}$, and $tA_{0,1}$ and $tA_{1,0}$, respectively. Rate constants associated with $tIni$, $tTerm$, $tA_{0,1}$, $tA_{1,0}$, and $tE_{j,j+1}$ are named k_I, k_T, k_{0I}, k_{10} , and $kE_{j,j+1}$, respectively.

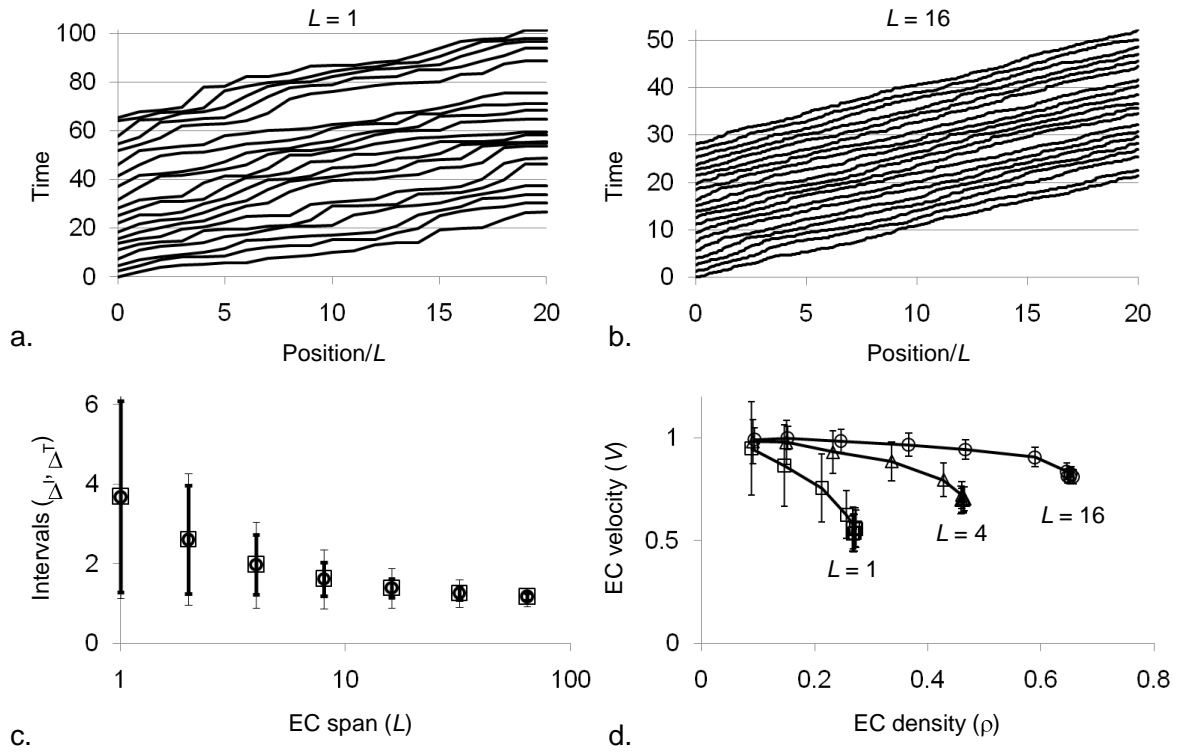


Figure 2. Effect of elongation complex (EC) span L on transcription rate. The track length was $20 \times L$, and the elongation rate k_E was L positions per unit of time in all simulations. The initiation rate (and thus the EC density) was maximal in all simulations except the ones in panel d. a, b: trajectories of the front of 20 ECs of span 1 and 16, respectively; note the different time scales. c: Average time intervals at steady state between initiation (circles) and termination events (squares), and their standard deviation (wider and narrower error bars for initiation and termination, respectively). d: Average steady state EC velocity (V) as a function of EC density on the track (ρ), for EC spans of 1, 4, and 16 positions. Variation in density was achieved by varying k_I .

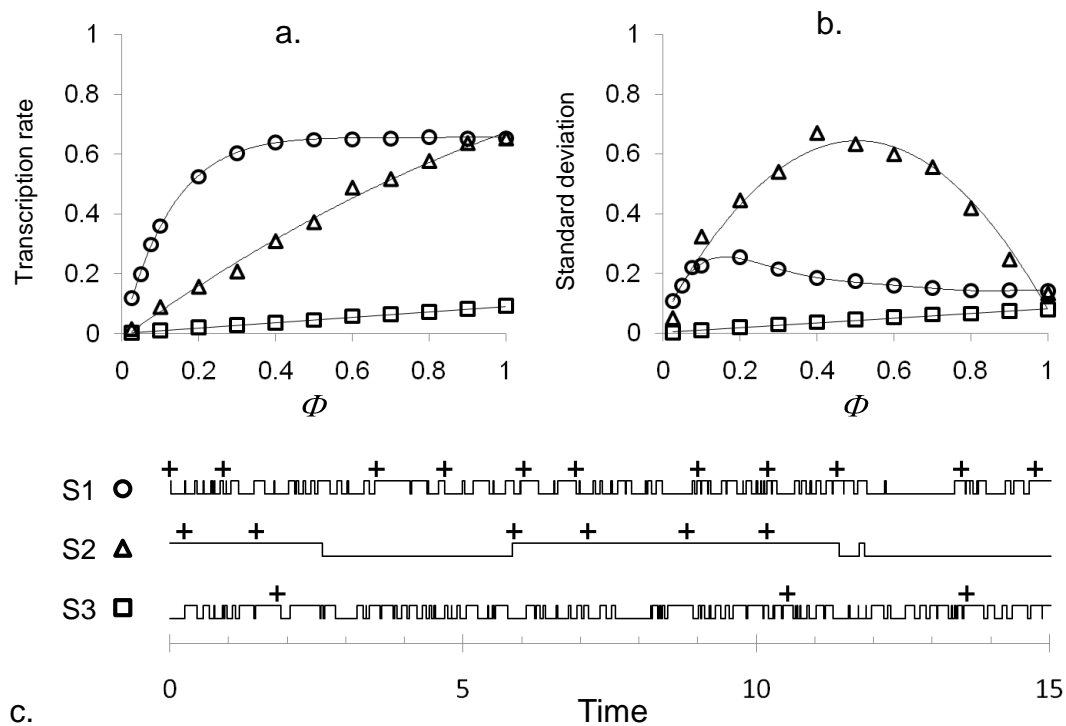


Figure 3. Mean observed steady state production rate (number of linear chains completed per unit of time, a) and its standard deviation (b) as a function of average activator binding site occupancy Φ (fraction of time the activation condition is true), and typical trajectories at $\Phi = 0.5$ (c) for S1, a responsive system that has efficient initiation (circles; $k_I = 10$ and $k_{I0} = 10$ per time unit), S2, an unresponsive system with efficient initiation (triangles; $k_I = 10$, $k_{I0} = 0.1$), and S3, a responsive system with inefficient initiation (squares; $k_I = 0.1$, $k_{I0} = 10$). All systems had an EC span L of 16 positions; a track length N of $20 \times L$ (320 positions), and elongation rate constant k_E of L positions per time unit. Statistics were obtained from at least 300 full transcription rounds per data point. Standard deviations were computed from the intervals between successive initiations. Solid lines in a and b are inserted solely to guide the eye. Solid lines in c show the activation condition (low, false, high, true); crosses indicate where a new transcription round is initiated (**tIni** firing).